

AD-A139 976

A PILOTED SIMULATOR INVESTIGATION OF DECOUPLING
HELICOPTERS BY USING A NO. (U) ARMY RESEARCH AND
TECHNOLOGY LABS MOFFETT FIELD CA AEROMECHAN.
G BOUNER ET AL. MAY 84

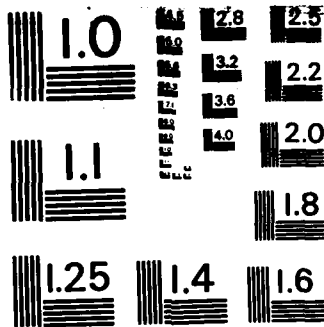
1/1

UNCLASSIFIED

F/G 1/3

NL





MICROCOPY RESOLUTION TEST CHART
NATIONAL BUREAU OF STANDARDS-1963-A

①

A PILOTED SIMULATOR INVESTIGATION OF DECOUPLING HELICOPTERS
BY USING A MODEL FOLLOWING CONTROL SYSTEM

Gerhard Bower
Deutsche Forschungs- und Versuchsanstalt fur Luft- und
Raumfahrt e.V. (DFVLR)
Institut fur Flugmechanik
Braunschweig, West Germany

Kathryn B. Hilbert
Aeromechanics Laboratory
U.S. Army Research and Technology Laboratories (AVSCOM)
NASA Ames Research Center
Moffett Field, California

AD A139976

PRESENTED AT THE 40TH ANNUAL FORUM
OF THE
AMERICAN HELICOPTER SOCIETY
ARLINGTON, VIRGINIA
MAY 16-18, 1984

DTIC FILE COPY

DTIC
ELECTE
APR 11 1984
S A D



All publishing rights reserved by the AHS, 217 N. Washington St., Alexandria, VA 22304

This document has been approved
for public release and sale; its
distribution is unlimited.

PAPER NO. A-84-40-07-4000

84 04 03 143

Table 1 Simulated BO-105 and UH-1H actuator characteristics

Axis	BO-105-S3		UH-1H V/STOLAND			
	Position limit, in. (%)	Rate limit, in./sec (%/sec)	Position limit, in. (%)		Rate limit, in./sec (%/sec)	
			Series	Parallel	Series	Parallel
Longitudinal	±6(100)	9(75)	±1.6(27)	±6(100)	11(92)	1.5(13)
Lateral	±6(100)	9(75)	±1.8(30)	±6(100)	12(100)	1.7(14)
Collective	0-10(100)	3(30)	±0.9(18)	0-10(100)	13.3(133)	0.9(9)
Pedals	±3.5(100)	3.5(50)	±0.9(26)	±3.5(100)	5.8(83)	0.9(13)

Table 2 Pilot experience

Pilot	Affiliation	Total flight hours			
		Helicopter	Fixed wing	BO-105	UH-1H
A	DFVLR	5300	400	900	2500
B	DFVLR	510	330	400	0

Table 3 Test matrix

Helicopter	Status	Actuating system	Task	
			60-knot dolphin	60-knot slalom
BO-105	Baseline	Ideal	Pilots A,B	Pilots A,B
	With MFCS	S-3	Pilots A,B	Pilots A,B
UH-1H	Baseline	Ideal	Pilot A	Pilot A
	With MFCS	V/STOLAND	Pilots A,B	Pilots A,B

Table 4 Averaged pilot ratings

HELICOPTER	STATUS	RATING									
BO-105	BASELINE										
	WITH MFCS										
UH-1H	BASELINE										
	WITH MFCS										
		1	2	3	4	5	6	7	8	9	10

HANDLING QUALITIES

HELICOPTER	STATUS	RATING									
BO-105	BASELINE										
	WITH MFCS										
UH-1H	BASELINE										
	WITH MFCS										
		1	2	3	4	5	6	7	8	9	10

PILOT WORKLOAD

HELICOPTER	STATUS	RATING									
BO-105	BASELINE										
	WITH MFCS										
UH-1H	BASELINE										
	WITH MFCS										
		1	2	3	4	5	6	7	8	9	10

TASK PERFORMANCE

TASK: 80 KNOT DOLPHIN



Accession For

NTIS GRA&I

DTIC TAB

Unannounced

Justification

Per Jim Cunniff

No contract No

Distribution/

Availability Codes

Avail and/or

Dist Special

A-1

**A PILOTED SIMULATOR INVESTIGATION OF DECOUPLING HELICOPTERS
BY USING A MODEL FOLLOWING CONTROL SYSTEM**

Gerhard Bower
Deutsche Forschungs- und Versuchsanstalt für Luft- und Raumfahrt e.V. (DFVLR)
Institut für Flugmechanik
Braunschweig, West Germany

Kathryn B. Hilbert
Aeromechanics Laboratory
U.S. Army Research and Technology Laboratories (AVSCOM)
NASA Ames Research Center
Moffett Field, California

Abstract

A U.S. and German piloted simulation experiment conducted to evaluate the performance of a model following control system by applying it to hingeless-rotor and teetering-rotor helicopters is reported. The explicit model was a linear, decoupled model such that the pilot commanded pitch attitude with the longitudinal cyclic, roll attitude with the lateral cyclic, yaw rate with the pedals, and Earth-fixed downward velocity with the collective. The results of the simulation indicate that the performance of the model following control system is primarily dependent on the limitations of the actuating system. Satisfactory handling qualities were achieved for both augmented helicopters flying two specified evaluation tasks: dolphin and slalom maneuvers. The significant improvements in task performance and handling qualities achieved for these two radically different helicopters, augmented with the designed model following control system, indicates the flexibility and versatility of this control technique.

Notation

A = helicopter dynamics matrix where $\dot{x} = Ax + Bu$
 B = helicopter control matrix
 C = model sensitivity matrix
 e = error between the helicopter state and model state
 G = control system matrices
 HP = power
 I = identity matrix
 J = rotor moment of inertia about shaft, slug-ft²

K = gain
 Q = torque, ft-lb
 r = yaw rate in the body-c.g. axes system, deg/sec
 s = Laplace transform variable
 T = sample time, sec
 \vec{u} = control vector, $\vec{u} = (\delta_e, \delta_a, \delta_c, \delta_p)^T$
 w = Earth-fixed vertical velocity, ft/sec
 w_f = fuel flow rate, lb/hr
 \vec{x} = helicopter state vector, $\vec{x} = (u, w, q, \theta, v, p, \psi, r)^T$
 \vec{x}_M = model state vector, $\vec{x}_M = (\theta_M, \phi_M, w_M, r_M)^T$
 z^{-1} = unit delay
 δ_a = lateral cyclic stick movement, positive to right, in.
 δ_c = collective control input, positive up, in.
 δ_e = longitudinal cyclic stick movement, positive aft, in.
 δ_p = pedal movement, positive right, in.
 $\Delta()$ = increment in ()
 θ = Euler pitch angle, deg
 τ = time constant, sec
 ϕ = Euler roll angle, deg
 Ω = rotor angular velocity, rad/sec
 $[]^{-1}$ = matrix inverse
 $[]^T$ = matrix transpose

Presented at the 40th Annual Forum of the American Helicopter Society, Crystal City, Virginia, May 16-18, 1984.

Subscripts

- c = commanded
- D = discretized
- E = engine
- M = model
- o = trim or reference condition
- R = required

Introduction

A joint research program between the Deutsche Forschungs- und Versuchsanstalt für Luft- und Raumfahrt e.V. (DFVLR) and the U.S. Army, under the Helicopter Flight Controls Memorandum of Understanding, was established to develop and evaluate model following control methods. The long-term objective of the program is to develop and implement a model following control system on a flight research facility for use in handling qualities, parameter identification, and control system experiments. The advantage of using a model following control system on a fly-by-wire helicopter is that the characteristics of the model to be followed can be varied quickly and easily depending on the desired task to be performed.

A model following control system was designed at the DFVLR, and a preliminary flight test program, using the MBB BO-105 S3 helicopter, was conducted to determine the feasibility of using such a control system for variable stability applications. Results of this experiment demonstrated that decoupling of the BO-105 was possible using the model following control system, and it was recommended that further research be conducted in this area.

Before undergoing more extensive flight test programs, a U.S./German piloted simulation experiment, the topic of this paper, was designed and conducted. The purpose of the experiment was to investigate the decoupling performance and limitations of the designed model following control system and to determine how easily it could be adapted to a new baseline helicopter, the NASA/Army variable stability UH-1H V/STOLAND. The BO-105 (hingeless rotor) and UH-1H (teetering rotor) helicopters were chosen because they have extreme differences in control system actuation, as well as in control power and flight dynamics corresponding to their different rotor systems. Two methods of assessing the decoupling performance of the model following control system were used in this simulation: pilot ratings

and a recently developed quantitative measure of model following performance. This paper discusses the results of the piloted portion of the experiment. Analysis of the model following control system using the new performance criterion will be reported in a subsequent paper.

Experiment Design

Mathematical Models

Simulation of the baseline helicopters was accomplished using two versions of a ten-degree-of-freedom, nonlinear, generic helicopter mathematical model.¹ One version of the mathematical model was configured to simulate the flight dynamic characteristics of the DFVLR BO-105 S3 helicopter and the other to simulate those of the NASA/Army UH-1H V/STOLAND helicopter without stabilizer bar.

To make possible the transfer of the simulation results to future flight test programs, the different actuating systems of these two variable-stability helicopters were also simulated. The fly-by-wire actuators of the BO-105 S3, shown in Fig. 1, are installed in all four axes and mechanically connected to the safety pilot's controls. These actuators are full-authority and quick in response. A simple second order model of the BO-105 fly-by-wire actuators was simulated for this experiment (Fig. 2). Because of limits in the hydraulic force booster, the rates of all the simulated actuators were constrained.

The UH-1H V/STOLAND actuating system utilizes a combination of a parallel servo and a series servo in the linkage of each control.² Figure 3 shows the servo installations for the cyclic controls. The series servos, which are severely limited in authority, are the faster responding actuators and thus act primarily on the transient behavior. The parallel actuators are full-authority rate servos which act to off-load the series servos and thus provide a trimming function. In addition, there are disconnect devices in the evaluation pilot's pitch and roll cyclic controls to allow for fly-by-wire operation. Figure 4 shows the simulated UH-1H V/STOLAND actuating system. The series servos were modeled by a second order filter, and the parallel servos were modeled by an integrator. If the series servo operates at its position limit, the gain K is used to force the parallel servo to operate at its maximum rate.

A comparison of the simulated actuator characteristics and limitations for the BO-105 and UH-1H is shown in Table 1. The

main limitations in the UH-1H actuating system are the limited-authority series servos. The main restriction in the BO-105 actuating system is the collective rate limit of 30%/sec. This limitation is primarily the result of the rotor rpm dynamics and limits. To represent accurately the influence of the rotor rpm on the model following control system, a simple model of the BO-105's engine and rpm governor was implemented in the simulation mathematical model. Figure 5a shows the standard rpm governor used in the ten-degree-of-freedom generic helicopter mathematical model (from Ref. 1). This model was modified for this simulation experiment based on actual DFVLR BO-105 flight test data (Fig. 5b). Several simplifying assumptions were made in deriving the block diagram shown in Fig. 5b from the one in Fig. 5a:

- 1) The throttle is held constant at 100%
- 2) The required torque, Q_R , is directly proportional to the pilot's collective stick input, δ_c
- 3) The relationship between engine power, HP, and engine torque, Q_E , is linear so that the engine produces engine torque directly from the change in fuel flow

Explicit Model

Previous research programs³⁻⁶ have demonstrated that the handling qualities of a helicopter flying typical mission scenarios can be improved if the interaxis coupling is minimized. Interaxis coupling, such as pitch-roll cross-coupling and collective input coupling to pitch and yaw, generally requires complex control coordination by the pilot in terrain flight and is, therefore, a major factor influencing the flying qualities of the helicopter.

Accordingly, the explicit model chosen for this experiment was a linear, decoupled model; the pilot commands pitch attitude with longitudinal cyclic, roll attitude with lateral cyclic, yaw rate with pedals, and Earth-fixed downward velocity with collective. A block diagram of the explicit model is shown in Fig. 6. The feedback and feed-forward matrices, A_M and B_M , are diagonal matrices for a decoupled model. The model time constants and sensitivities were determined in pre-simulation checkout and adjusted, based on pilot comments, to give good handling qualities. A special turn coordination feature was included in the model. The turn coordination feature attempts to minimize lateral acceleration in turns above

20 knots by commanding both roll angle and yaw rate with the lateral cyclic stick.

Model Following Control System

In a typical model following control system (MFCS) (Fig. 7) the pilot's commands are disconnected from the actual aircraft and fed into a model. This model may, for example, be the equations of motion of an aircraft to be investigated or the dynamics of a system with good handling qualities. The errors between the states of the model and those of the base system are fed into the control system, which attempts to minimize the state errors by generating control signals for the actuators. If the state errors are always zero, the controlled vehicle exhibits the dynamics of the model.

The main objective of the designed MFCS shown in Fig. 8 is to control the attitudes to be followed in the outer loop by controlling the rates in the inner loop. The feedback matrices, G_1 and G_2 , are used by the designer to select the desired outer-loop and inner-loop states to be controlled. The elements of G_1 and G_2 are either 1's or 0's, and each matrix contains a maximum of four elements equal to 1 (the number of states to be followed must equal the number of controls available). Once G_1 and G_2 are defined, the controller matrix G_c is dependent only on the base system's control matrix B_D for the four commanded variables. The controllers used are feed-forward gains calculated using a nonreal-time identification procedure which incorporates a linearized version of the actual helicopter. In addition, the elements of the controller matrix are adjusted with air-speed to improve the accuracy and robustness of the system. The output of the controller matrix is integrated to suppress constant errors and hold the base system in the trim state over the whole flight envelope. It was found that in cases in which either the rate or position limit of one of the four actuators is exceeded, the error between the controlled state and the actual helicopter state can build up very quickly and cause instabilities owing to saturated integrators. This instability problem was overcome by stopping the integration of the controller output for the axis in which the actuator is limited by zeroing the corresponding element of the diagonal G_c matrix. Finally, the elements of the diagonal G_c are used to convert the attitude errors to a specified amount of commanded rate.

Initially, the controller matrix G_c was equal to the inverse of the base helicopter's control matrix B_D . However, for

tasks requiring large and rapid control inputs where the rate or position limits of one or more of the actuators is exceeded, this linear control system causes overcontrolling in the unlimited axes. For this case of limited actuators, an optimal control law was developed:

$$\vec{u}_{\text{unlimited}} = (B_1^T B_1)^{-1} B_1^T (\vec{e} - B_D(i,3) \vec{u}_{\text{limited}})$$

$B_D(i,3)$: third column of matrix B_D (1)

In Eq. (1), B_1 denotes the base system's control matrix corresponding to the unlimited portion of the control vector. The optimal control law minimizes all four state errors using only the unlimited controls while holding the limited controls at either the maximum rate or position. The controller matrix G_1 is redefined as the pseudo-inverse of the matrix B_1 :

$$G_1 = (B_1^T B_1)^{-1} B_1^T \quad (2)$$

An example calculation of the controller matrix G_1 for the BO-105 in 60-knot level flight is given in the Appendix.

To illustrate the difference between the linear control system and the linear control system plus the controller optimization feature, Fig. 9 shows the response of the BO-105, augmented with the two different control systems, to a 3-2-1-1 collective stick input of 1.0-in. magnitude during 60-knot level flight. Figure 9a shows the collective input and corresponding response of the collective actuator. For this input, the MFCS commands a vertical velocity of ± 8 ft/sec, filtered with a frequency of 1.67 rad/sec. In addition, the MFCS attempts to hold the three other states at their 60-knot trim positions through manipulation of their actuator positions. It can be seen that the collective actuator was rate-limited during a considerable portion of the input. Figure 9b shows the time histories for the four helicopter states for both the linear control system and the optimized linear control system. As expected, errors between the desired model states and the helicopter states occur when the collective actuator is operating at its rate limit. Maximum errors of $10^\circ/\text{sec}$, 4° , and 3° in yaw rate, pitch attitude, and roll attitude, respectively, were observed for the linear control system. The advantage of the linear control system with the controller optimization feature is apparent in the decrease in interaxis coupling, particularly the collective-to-yaw-rate coupling.

Conduct of the Experiment

Facility Description

This experiment was conducted on a fixed-base simulator at Ames Research Center. The simulator facility includes a single-seat cockpit cab equipped with conventional helicopter controls and a typical instrument panel (Fig. 10). Switches in the simulator cab were used by the pilots to enable the various features of the control system. A 600:1 scale terrain board and camera visual system depicting a runway with two 100-ft obstacles positioned on the centerline (Fig. 11) was presented through the cab window on a color television monitor with a collimating lens.

Evaluation Task Description

Evaluation of the model following control system for the two helicopters under investigation was accomplished using two typical nap-of-the-Earth mission tasks: a dolphin (Fig. 12) and a slalom (Fig. 13) task. The dolphin task required the pilot to fly over two 100-ft obstacles spaced 1150 ft apart while attempting to maintain a 60-knot airspeed and an altitude of 75 ft between the obstacles. The control strategy the pilots were instructed to follow was to use primarily collective stick inputs to perform the task and to minimize deviations in airspeed, heading, pitch attitude, and roll attitude with the remaining three controls. The slalom task was a lateral avoidance task which required the pilot to maneuver around 100-ft high obstacles spaced 1150 ft apart on the runway centerline while maintaining altitude (75 ft AGL) and airspeed (60 knots).

Evaluation Pilots' Background and Experience

Two DFVLR pilots participated as evaluation pilots in this simulation study. A summary of their flight time is presented in Table 2.

Data Acquisition

Pilot evaluation data, time histories, and magnetic tape recordings of specified flight parameters were collected. Variables recorded included pilot control inputs, actuator positions, model attitudes and rates, helicopter attitudes and rates, airspeed, torque, and rotor rpm. The pilot evaluation data consist of Cooper-Harper handling qualities ratings⁷ and two additional ratings: one of pilot workload and stress and the other of overall quality of the task performance. These ratings were obtained using a modified Cooper-Harper rating scale (Fig. 14),

developed and used at the DFVLR (Ref. 8); they are used to give more insight into the secondary factors affecting the pilot during the task. In addition to the three ratings, the pilots were asked to provide written commentary to help identify those aspects of the system that most heavily influenced the ratings.

Test Matrix

The test matrix for this experiment is shown in Table 3. Evaluation of the baseline helicopter without the model following control system was done assuming an ideal actuating system (no rate or position limits). Generally, only one task was performed by the pilot in a typical simulation session. Three evaluation runs per pilot were collected for each task. As indicated in the test matrix, the pilots evaluated the baseline helicopter (without MFCS) for both tasks first and then evaluated the augmented helicopter (with MFCS).

Other Experimental Considerations

A significant amount of simulation time was allotted for pilot familiarization with the simulation facility and simulated helicopters. In order to minimize pilot learning-curve effects, evaluation data were not collected until the pilots demonstrated a consistent level of proficiency with the system. In general, it took the pilots a great deal more time to become familiar with the baseline helicopter than with the baseline helicopter augmented with the MFCS. Using the extensive pilot familiarity and experience with the actual MBB BO-105 helicopter, the dynamics of the simulated baseline BO-105 were adjusted to match the actual BO-105 before any evaluation data were collected. This adjustment was not done with the simulated UH-1H since the pilots were not familiar with the characteristics of the UH-1H without its stabilizer bar.

Results

Since the decoupling effects of the model following control system are more pronounced in the dolphin task, time histories and pilot ratings of that task are used to illustrate the major results. Similar results and trends were observed for the slalom task.

Figure 15 illustrates the effects on pilot's control activity for the 60-knot dolphin task when augmenting the BO-105 with the MFCS. On the left are shown the required control positions for the unaugmented BO-105. As instructed, the pilot used the collective stick as the primary

control in flying the task. The pedals were used as a secondary control to minimize the collective-to-yaw-rate coupling. Longitudinal cyclic inputs were made to minimize collective-to-pitch coupling which necessitated lateral cyclic inputs to compensate for pitch-roll coupling. On the right are shown the four control positions for the BO-105 augmented with the MFCS performing the identical dolphin. These time histories indicate that the pilot needed only the collective control to perform the task.

A comparison of the BO-105's states, with and without the MFCS, during these same dolphin evaluation runs is shown in Fig. 16. In general, the criterion for acceptable model following performance is based on the error between the commanded and measured response. Maximum errors of 5°/sec in yaw rate, 7.2° in pitch attitude, and 9.6° in roll attitude were observed for the unaugmented BO-105. These errors reduced to 2.4°/sec, 1.8°, and 3° in yaw rate, pitch attitude, and roll attitude, respectively, for the augmented BO-105. In addition, the airspeed errors went from 5 knots in the uncontrolled case to nearly 0 knots in the controlled case. This result shows that without wind and turbulence, the desired flightpath and 60-knot airspeed were held constant, even though those parameters were not commanded directly by the MFCS.

Figure 17 shows the difference in the control system activity needed to decouple the BO-105 and UH-1H for the 60-knot dolphin task. The BO-105's actuator positions are strikingly similar to the pilot's control activity for the uncontrolled BO-105 shown in Fig. 15. Following a control strategy similar to that used by the pilots, the MFCS uses the collective actuator as the primary control and the pedal actuator as a secondary control in performing the task. Longitudinal and lateral cyclic actuators are used to minimize interaxis coupling.

For the UH-1H, the activity of the four series servos is shown since these are more demanding on the control system than the parallel servos. Because the UH-1H simulation model did not include the stabilizer bar, the dynamics and controllability of the helicopter were severely degraded. The strong coupling between collective inputs and pitch rate exhibited by the simulated uncontrolled UH-1H is very apparent in the response of the longitudinal series servo position. High activity in all four series servos was required in order to decouple the strongly coupled and extremely nonlinear dynamics of this helicopter.

Table 4 summarizes the averaged pilot ratings in handling qualities, pilot workload, and task performance for the dolphin task. These results should not be interpreted as constituting a comparison of the handling qualities of the BO-105 and the UH-1H. Rather they should be interpreted as a comparison of the baseline simulation mathematical model with and without the designed model following control system.

Both pilots commented on the lack of visual information for height and rate of descent. They found it particularly difficult to estimate the point over the hurdles at which the descent should be initiated.

Both pilots considered the baseline UH-1H mathematical model uncontrollable and unflyable (pilot rating of 10) for the 60-knot dolphin task. This result was attributed to the high couplings and low dynamic stability of the simulated vehicle without the stabilizer bar. The baseline BO-105 received only adequate ratings, a result of the strong couplings, collective-to-yaw and collective-to-pitch, which made it difficult to hold airspeed and heading. In addition, attempts by the pilot to minimize airspeed deviations between the hurdles created lateral deviations and, therefore, increased pilot workload.

Satisfactory ratings in all three categories were achieved when the MFCS was added to both baseline helicopters. The improvement in the handling qualities is primarily a result of the decrease in the pilot's control activity and, therefore, workload, as illustrated in Fig. 15. For the BO-105, the addition of the MFCS improved pilot ratings 3 points for handling qualities, 5 points for pilot workload, and 4.5 points for task performance. Pilot ratings of 1 were achieved in all three categories for the augmented UH-1H. The simulated UH-1H helicopter went from

being a totally uncontrollable vehicle in the baseline configuration to one that exhibited excellent handling qualities, allowing satisfactory task performance with minimal pilot workload, with the addition of the MFCS. This drastic change in ratings demonstrates the ability of the designed model following control system to decouple a helicopter.

Conclusions

A new model following control technique has been developed for potential application to a variable-stability helicopter. Presented in this paper are some of the results of a fixed-base simulation experiment which evaluated the performance and limitations of this control system when used to make large changes in the response characteristics of two very different helicopters, the BO-105 and the UH-1H. The helicopters were evaluated, with and without the MFCS, for a 60-knot dolphin task and a 60-knot slalom task. The following general tendencies and conclusions are noted:

- 1) The changes in response characteristics resulted in significant improvements in the performance and handling qualities of both vehicles, flying typical nap-of-the-Earth mission tasks, because of a substantial decrease in interaxis coupling and, therefore, less pilot control activity and workload.
- 2) Optimization of the control laws was required to improve the model following performance in situations in which the actuators are position or rate limited.
- 3) The flexibility and simplicity of the model following control system design allows for quick and easy adaptation to helicopters with different dynamic characteristics and actuating systems.

Appendix

Control System Design Example: BO-105 in 60-knot Level Flight

Step 1: Equations of motion: $\dot{x} = Ax + Bu$

$$A = \begin{bmatrix} -0.0322 & 0.0210 & 2.5125 & -32.1990 & 0.0018 & -0.5693 & 0.0000 & -0.0319 \\ -0.0534 & -0.7974 & 1.1900 & -0.2019 & -0.0043 & -1.6577 & 0.9670 & -0.1329 \\ 0.0135 & 0.0003 & -4.0010 & 0.0000 & -0.0025 & 2.2435 & 0.0000 & 0.1145 \\ 0.0000 & 0.0000 & 0.9995 & 0.0000 & 0.0000 & 0.0000 & 0.0000 & 0.0300 \\ 0.0026 & -0.0056 & -0.5699 & 0.0061 & -0.1440 & -2.7438 & 32.1850 & 0.9100 \\ -0.0046 & -0.0021 & -5.9050 & 0.0000 & -0.0689 & -10.0650 & 0.0000 & 0.1432 \\ 0.0000 & 0.0000 & -0.0002 & 0.0000 & 0.0000 & 1.0000 & 0.0000 & 0.0063 \\ -0.0052 & -0.0090 & 0.1708 & 0.0000 & 0.0402 & -0.0085 & 0.0000 & -0.8351 \end{bmatrix}$$

Step 1 (contd)

$$B = \begin{bmatrix} -0.7507 & -0.0129 & 0.0994 & 0.0276 \\ -1.9859 & 0.3991 & -8.4075 & 0.0277 \\ 1.0243 & 0.0627 & 0.2892 & 0.0210 \\ 0.0000 & 0.0000 & 0.0000 & 0.0000 \\ -0.0096 & 0.7165 & -0.0505 & -1.7734 \\ -0.1913 & 2.3651 & -0.1032 & -1.0503 \\ 0.0000 & 0.0000 & 0.0000 & 0.0000 \\ -0.0282 & 0.0298 & 0.2243 & 1.5009 \end{bmatrix}$$

Step 2: Discretize the equations of motion using the backward rectangular z-transform: $x[i+1] = A_D x[i] + B_D u[i]$

$$B_D = \begin{bmatrix} -0.2230 & -0.0510 & -0.0082 & 0.0086 \\ -0.3074 & 0.0420 & -1.4411 & 0.0128 \\ 0.1005 & 0.0417 & 0.0283 & -0.0098 \\ 0.0201 & 0.0084 & 0.0059 & -0.0004 \\ -0.0502 & 0.2363 & -0.0161 & -0.3411 \\ -0.0518 & 0.1396 & -0.0173 & -0.0619 \\ -0.0104 & 0.0279 & -0.0034 & -0.0121 \\ -0.0015 & 0.0077 & 0.0414 & 0.2546 \end{bmatrix}$$

$$= (I - A \cdot T)^{-1} \cdot B \cdot T$$

Sample time of MFCS $T = 0.2$ sec

Step 3: Retain only the four desired rows of B_D to achieve a square matrix - convert the angle measurements from radians to degrees.

The resulting controller matrix is

$$G_1 = \begin{bmatrix} 0.3987 & 0.1428 & -0.0808 & 0.0111 \\ -0.1209 & 0.2655 & 0.0334 & -0.0142 \\ 0.1015 & 0.0187 & -0.3675 & 0.0598 \\ -0.0052 & 0.0128 & 0.0018 & 0.0336 \end{bmatrix}$$

$$= (r \cdot B_D^{-1})^T$$

$$r = 0.5$$

where r is a correction factor to optimize the control activity versus the control system performance.

Step 4: For the case in which the collective actuator is operating at its rate limit, modify B_D

$$B_1 = \begin{bmatrix} 1.1511 & 0.4806 & -0.0241 \\ -0.5937 & 1.6006 & -0.6912 \\ -0.3074 & 0.0420 & 0.0128 \\ -0.0850 & 0.4432 & 14.5901 \end{bmatrix}$$

Step 5: The controller matrix is redefined as the pseudo-inverse of B_1

$$G_1 = \begin{bmatrix} 0.3571 & -0.1037 & -0.0879 & -0.0042 \\ 0.1375 & 0.2677 & -0.0058 & 0.0129 \\ -0.0021 & -0.0088 & -0.0002 & 0.0339 \end{bmatrix}$$

$$= r[(B_1^T B_1)^{-1} B_1^T]$$

Acknowledgments

The authors gratefully acknowledge the contributions of simulation applications engineer, R. Leeper, and the services of the two participating pilots, K. Sanders and M. Roessing.

References

¹Talbot, P. D., Tinling, B. E., Decker, W. A., and Chen, R. T. N., "A Mathematical Model of a Single Main Rotor Helicopter for Piloted Simulation," NASA TM-84281, 1982.

²Baker, F. A., Jaynes, D. N., Corliss, L. D., Liden, S., Merrick, R. B., and Dugan, D. C., "V/STOLAND Avionics System Flight-Test Data on a UH-1H Helicopter," NASA TM-78591, 1980.

³Chen, R. T. N., "Unified Results of Several Analytical and Experimental Studies of Helicopter Handling Qualities in Visual Terrain Flight," Helicopter Handling Qualities, NASA CP-2219, 1982.

⁴Pausder, H.-J. and Hummes, D., "Flight Tests for the Assessment of Task Performance and Control Activity," Helicopter Handling Qualities, NASA CP-2219, 1982.

⁵Corliss, L. D. and Carico, G. D., "A Preliminary Flight Investigation of Cross-Coupling and Lateral Damping for Nap-of-the-Earth Helicopter Operations," Preprint No. 81-28, 37th Annual National Forum of the American Helicopter Society, New Orleans, La., May 1981.

⁶Chen, R. T. N., "Selection of Some Rotor Parameters to Reduce Pitch-Roll Coupling of Helicopter Flight Dynamics," Preprint No. I-6, National Specialists Conference on Rotor Systems Design of the American Helicopter Society, Philadelphia, Pa., Oct. 1980.

⁷Cooper, G. E. and Harper, R. P., Jr., "The Use of Pilot Ratings in the Evaluation of Aircraft Handling Qualities," NASA TN D-5153, 1969.

⁸Sanders, K., Pausder, H.-J., and Hummes, D., "Flight Tests and Statistical Data Analysis for Flying Qualities Investigations," Paper No. 56, 6th European Rotorcraft and Powered Lift Aircraft Forum, Bristol, England, Sept. 1980.

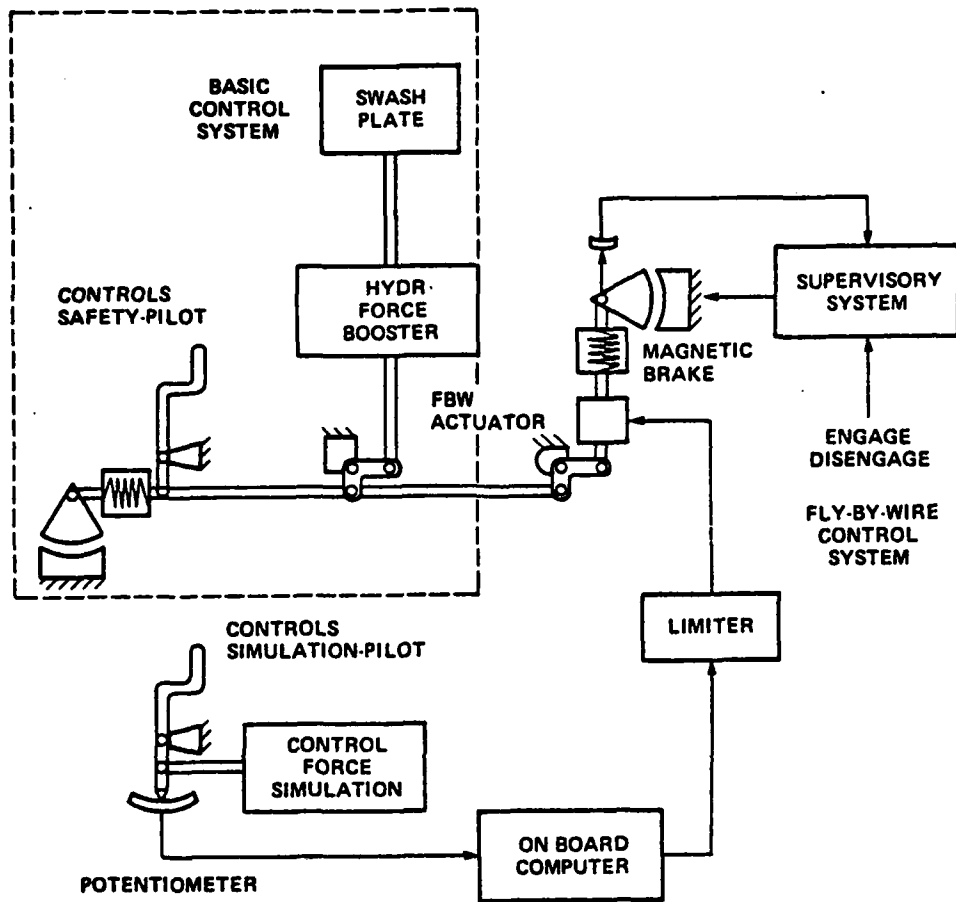


Fig. 1 BO-105 S3 control system.

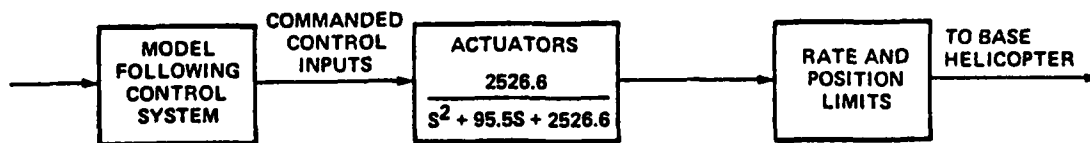


Fig. 2 Simulated BO-105 S3 actuator dynamics.

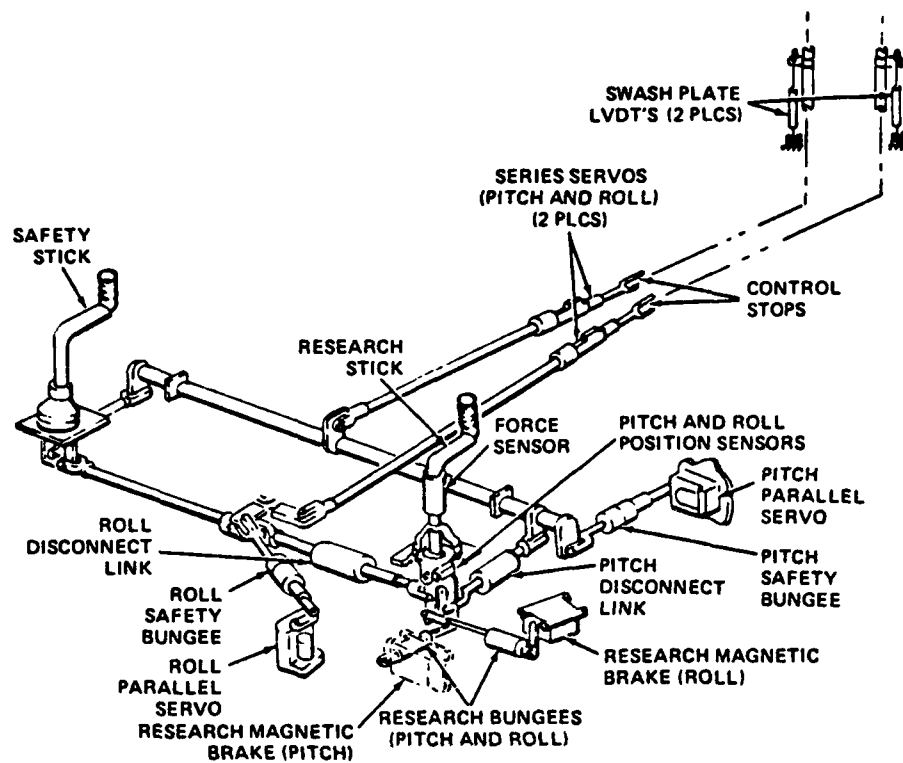


Fig. 3 UH-1H V/STOLAND control system longitudinal and lateral cyclic controls.

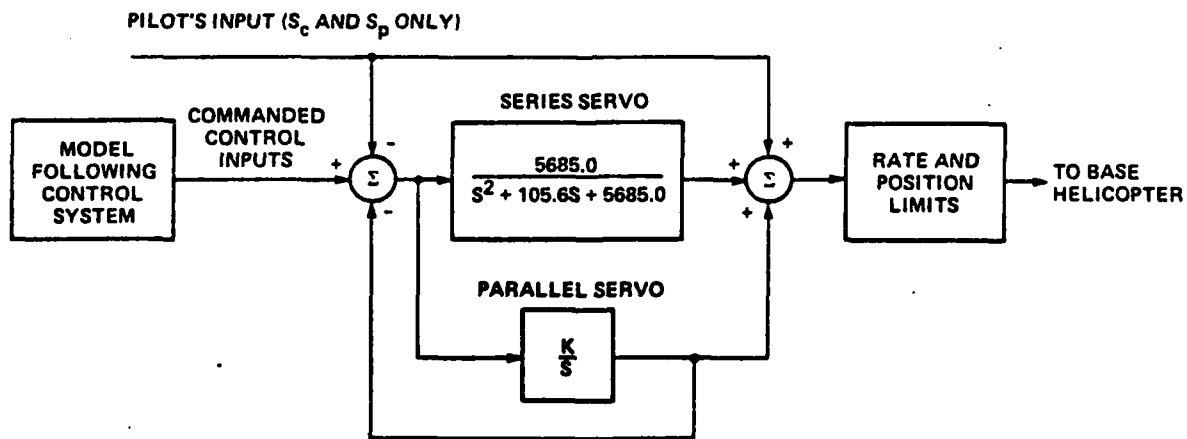
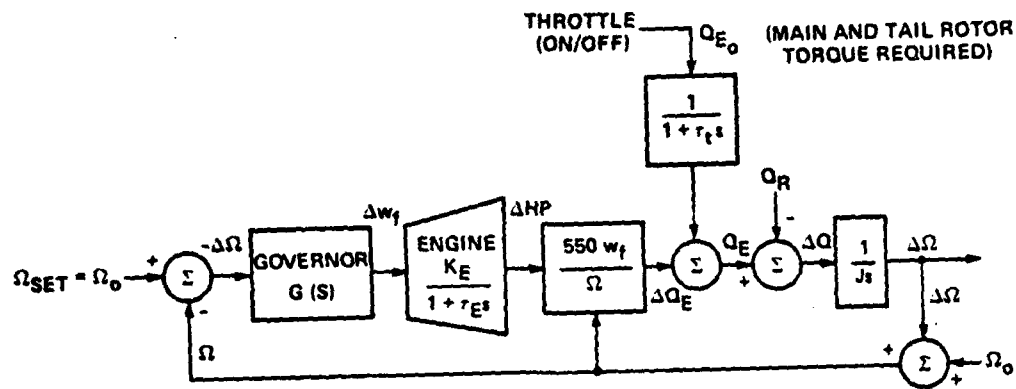
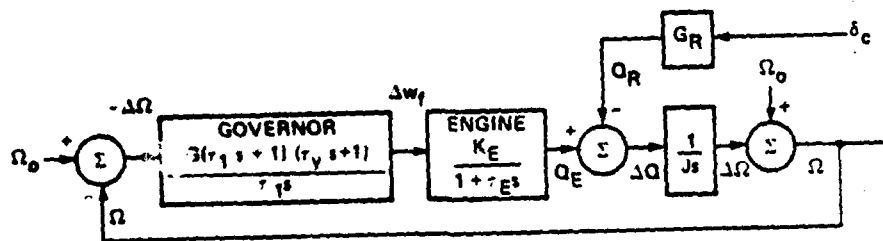


Fig. 4 Simulated UH-1H V/STOLAND actuating system.

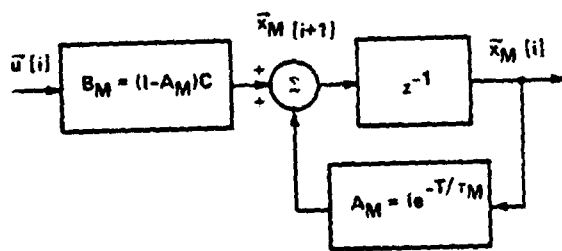


(a)



(b)

Fig. 5 RPM governor. a) Generic; b) simulated.



MODEL TIME CONSTANT: $\tau_M = 1.0 \text{ sec}$ (IN ALL FOUR AXES)

MODEL SENSITIVITY MATRIX: $C = \begin{bmatrix} 5.0 & 0 & 0 & 0 \\ 0 & 20.0 & 0 & 0 \\ 0 & 0 & -8.0 & 0 \\ 0 & 0 & 0 & 5.0 \end{bmatrix}$

Fig. 6 Explicit model.

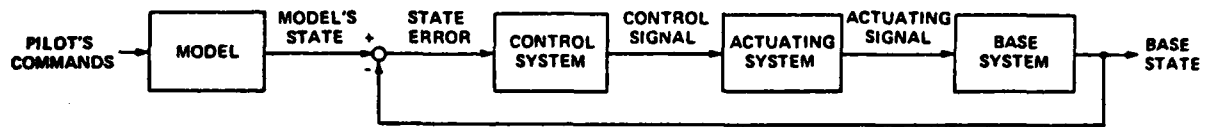
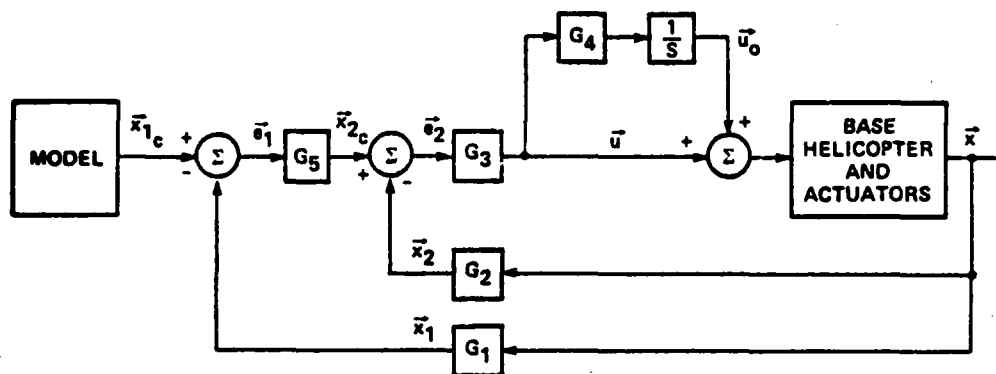


Fig. 7 Basic model following control system concept.



EXAMPLE: BO - 105 IN 60 knot LEVEL FLIGHT

$$\bar{x}_1 = [\theta, \phi, 0, 0]^T$$

$$G_1 = \begin{bmatrix} 0 & 0 & 0 & 1 & 0 & 0 & 0 \\ 0 & 0 & 0 & 0 & 0 & 1 & 0 \\ 0 & 0 & 0 & 0 & 0 & 0 & 0 \\ 0 & 0 & 0 & 0 & 0 & 0 & 0 \end{bmatrix}$$

$$G_3 = \begin{bmatrix} 0.400 & 0.143 & -0.082 & 0.011 \\ -0.121 & 0.266 & 0.037 & -0.014 \\ 0.102 & 0.019 & -0.368 & 0.060 \\ -0.005 & 0.013 & 0.002 & 0.034 \end{bmatrix}$$

$$G_5 = \begin{bmatrix} 1 & 0 & 0 & 0 \\ 0 & 1 & 0 & 0 \\ 0 & 0 & 1 & 0 \\ 0 & 0 & 0 & 1 \end{bmatrix}$$

$$\bar{x}_1 = [0, 0, w, r]^T$$

$$G_2 = \begin{bmatrix} 0 & 0 & 0 & 0 & 0 & 0 & 0 & 0 \\ 0 & 0 & 0 & 0 & 0 & 0 & 0 & 0 \\ 0 & 1 & 0 & 0 & 0 & 0 & 0 & 0 \\ 0 & 0 & 0 & 0 & 0 & 0 & 0 & 1 \end{bmatrix}$$

$$G_4 = \begin{bmatrix} 0.05 & 0 & 0 & 0 \\ 0 & 0.2 & 0 & 0 \\ 0 & 0 & 0.2 & 0 \\ 0 & 0 & 0 & 0.3 \end{bmatrix}$$

Fig. 8 Model following control system.

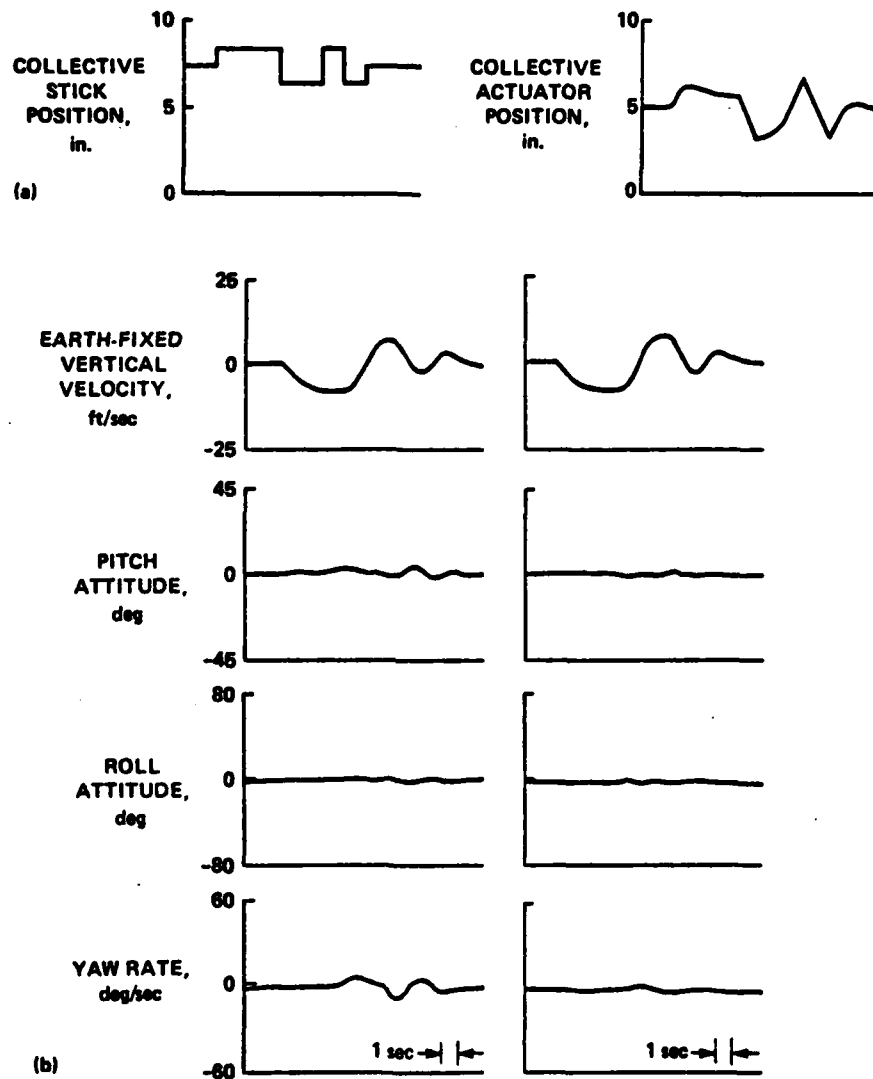


Fig. 9 Comparison of linear control systems for BO-105 at 60 knots. a) 1-in. 3-2-1-1 collective stick input and collective actuator response; b) linear control system vs optimized linear control system.



Fig. 10 Simulator cockpit and instrument panel.

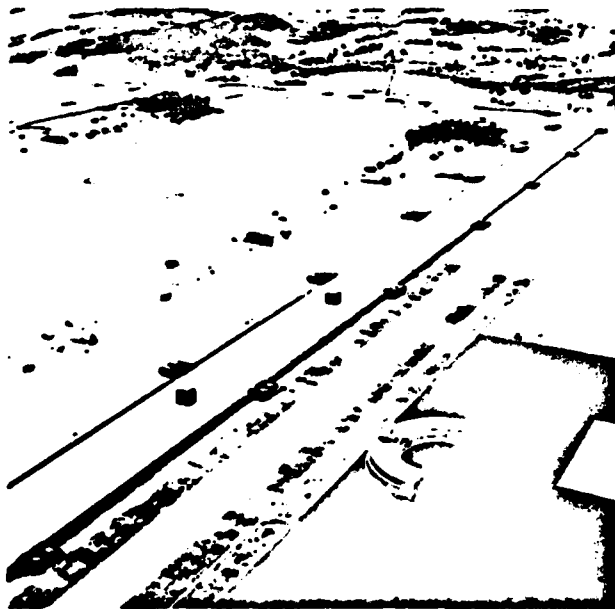


Fig. 11 Terrain board model.

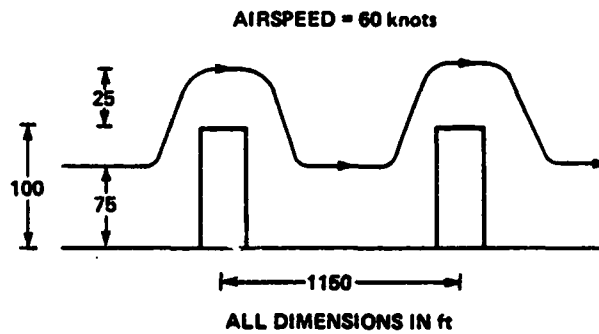


Fig. 12 Dolphin task.

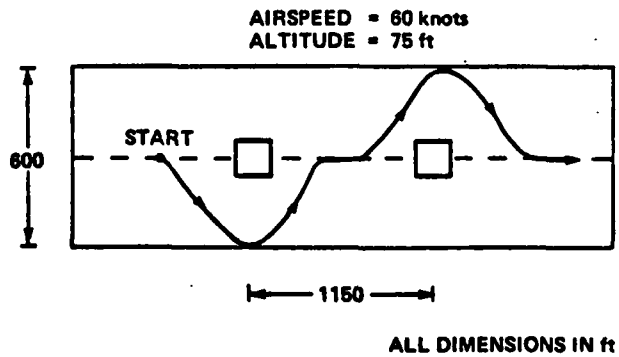


Fig. 13 Slalom task.

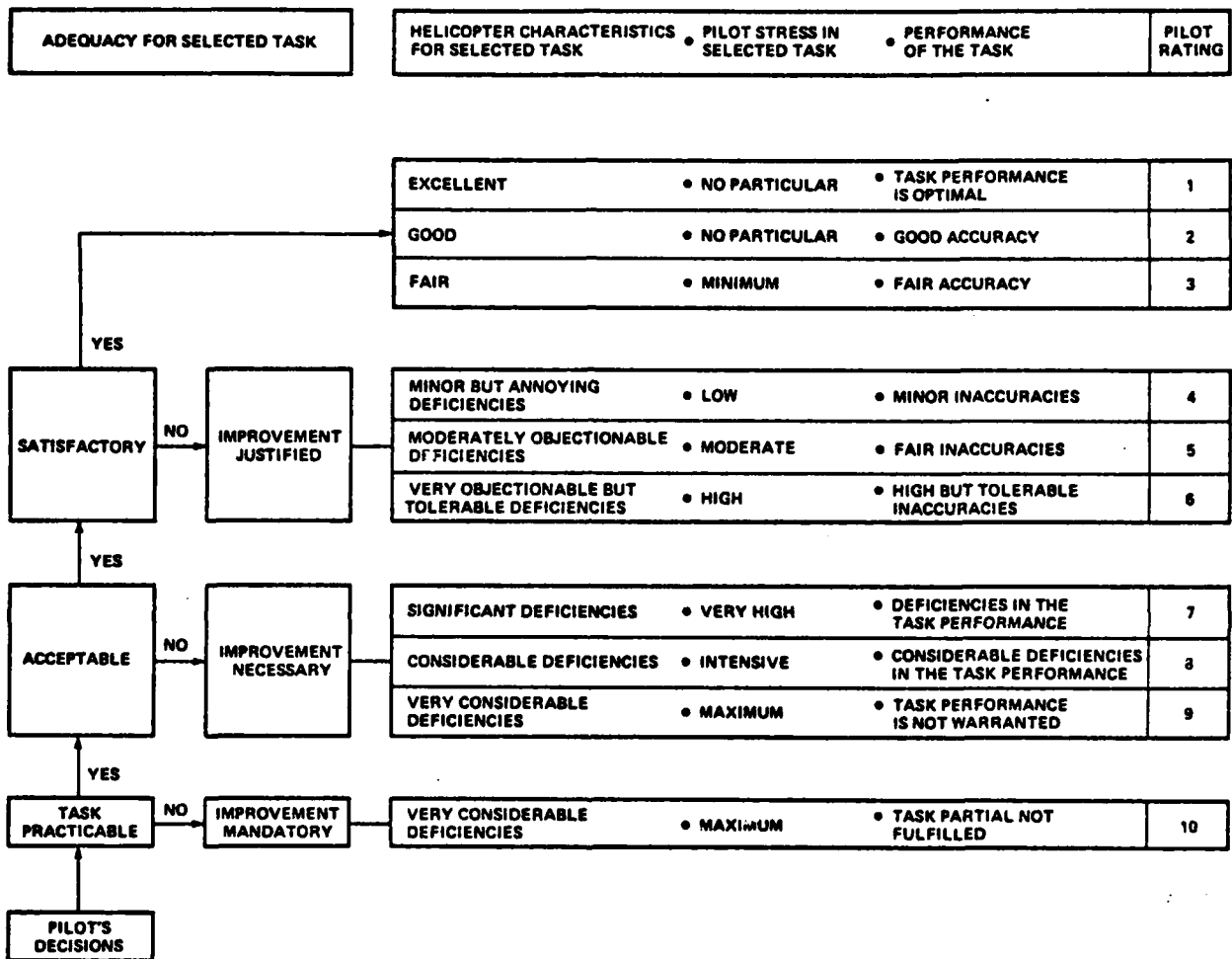


Fig. 14 Pilot stress and task performance rating scale.

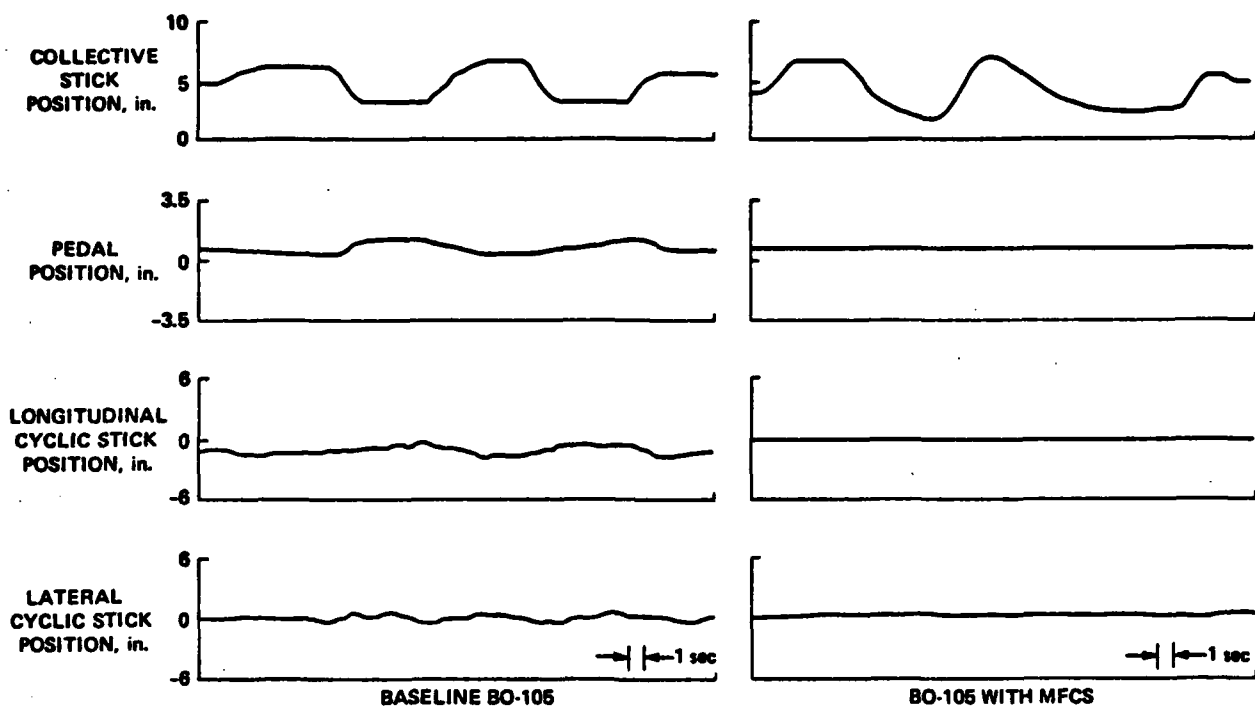


Fig. 15 Comparison of pilot's control activity: 60-knot dolphin.

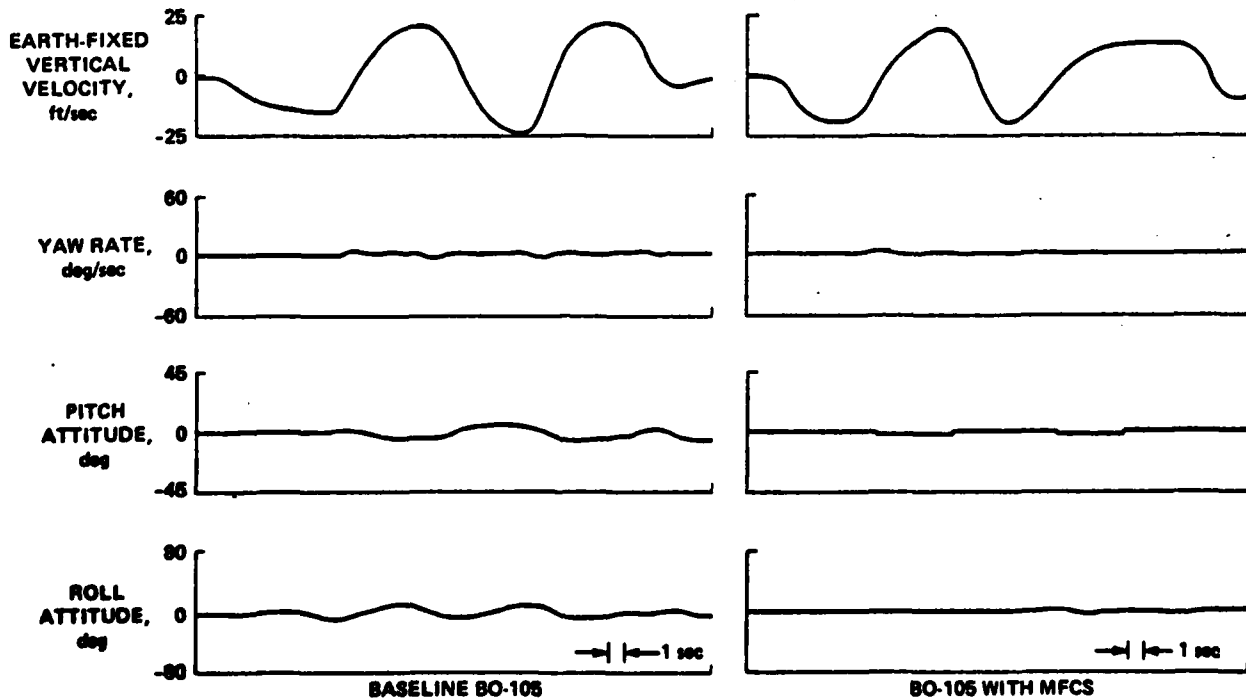


Fig. 16 Comparison of states: 60-knot dolphin.

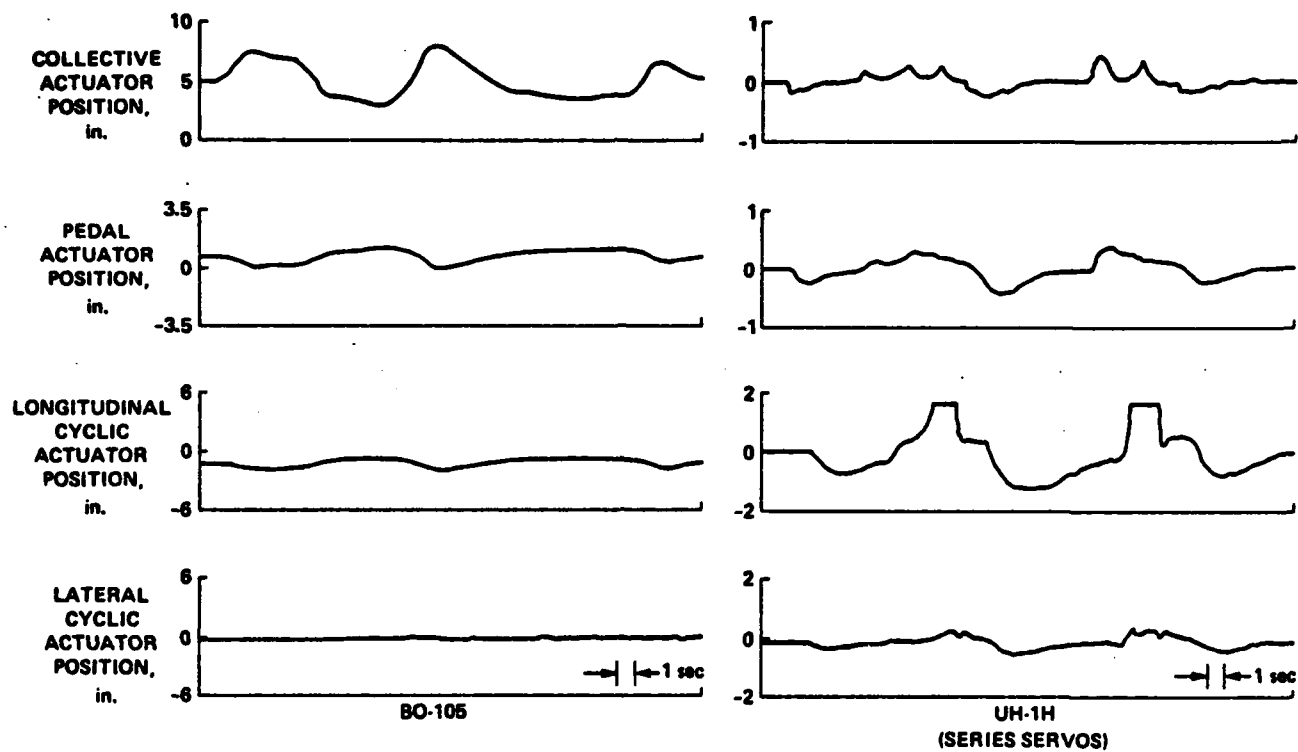


Fig. 17 Comparison of model following control system activity: 60-knot dolphin.

END

FILMED

5-84

DTIC